Heliyon 10 (2024) e26062

Contents lists available at ScienceDirect

Heliyon

journal homepage: www.cell.com/heliyon

Research article

Identification of immune infiltration and immune-related biomarkers of periprosthetic joint infection

Zhuo Li [a,b,c,e,1], Zhi-Yuan Li [a,b,1], Zulipikaer Maimaiti [b,f,1], Fan Yang [a,b,c], Jun Fu [b,d], Li-Bo Hao [b,d], Ji-Ying Chen [a,b,c,2,**], Chi Xu [b,d,2,*]

[a] Medical School of Chinese PLA, Beijing, China
[b] Department of Orthopedics, The First Medical Center, Chinese PLA General Hospital, Beijing, China
[c] School of Medicine, Nankai University, Tianjin, China
[d] Department of Orthopedics, The Fourth Medical Center, Chinese PLA General Hospital, Beijing, China
[e] Department of Joint Surgery, Shandong Provincial Hospital Affiliated to Shandong First Medical University, Jinan, Shandong, China
[f] Department of Orthopedics, Beijing Luhe Hospital, Capital Medical University, Beijing, China

ARTICLE INFO

Keywords:
Periprosthetic joint infection
Periprosthetic tissue
Biomarker
Immune infiltration
WGCNA

ABSTRACT

Background: The immune response associated with periprosthetic joint infection (PJI) is an emerging but relatively unexplored topic. The aim of this study was to investigate immune cell infiltration in periprosthetic tissues and identify potential immune-related biomarkers.
Methods: The GSE7103 dataset from the GEO database was selected as the data source. Differentially expressed genes (DEGs) and significant modular genes in weighted correlation network analysis (WGCNA) were identified. Functional enrichment analysis and transcription factor prediction were performed on the overlapping genes. Next, immune-related genes from the ImmPort database were matched. The protein-protein interaction (PPI) analysis was performed to identify hub genes. CIBERSORTx was used to evaluate the immune cell infiltration pattern. Spearman correlation analysis was used to evaluate the relationship between hub genes and immune cells.
Results: A total of 667 DEGs were identified between PJI and control samples, and 1847 PJI-related module genes were obtained in WGCNA. Enrichment analysis revealed that the common genes were mainly enriched in immune and host defense-related terms. TFEC, SPI1, and TWIST2 were the top three transcription factors. Three hub genes, *SDC1*, *MMP9*, and *IGF1*, were identified in the immune-related PPI network. Higher levels of plasma cells, $CD4^{+}$ memory resting T cells, follicular helper T cells, resting mast cells, and neutrophils were found in the PJI group, while levels of M0 macrophages were lower. Notably, the expression of all three hub genes correlated with the infiltration levels of seven types of immune cells.
Conclusion: The present study revealed immune infiltration signatures in the periprosthetic tissues of PJI patients. *SDC1*, *MMP9*, and *IGF1* were potential immune-related biomarkers for PJI.

* Corresponding author. Department of Orthopedics, The First Medical Center, Chinese PLA General Hospital, Beijing, China.
** Corresponding author. Department of Orthopedics, General Hospital of People's Liberation Army, Beijing, China.
E-mail addresses: jiyingchen_301@163.com (J.-Y. Chen), zhenyunale@163.com (C. Xu).
[1] These authors contributed equally to this work and share first authorship.
[2] These authors contributed equally to this work and share last authorship.

https://doi.org/10.1016/j.heliyon.2024.e26062
Received 4 July 2023; Received in revised form 6 February 2024; Accepted 7 February 2024
Available online 8 February 2024

1. Introduction

Periprosthetic joint infection (PJI) is a feared complication following total joint arthroplasty (TJA) and places a significant financial burden on the healthcare system due to its complex treatment strategy. Although PJI occurs in only about 1–3% of TJA cases, the growing number of TJA procedures makes it an increasingly important issue to address [1]. Unfortunately, the surgical failure rates for PJI remain high, ranging from 10 to 20% for two-stage exchange arthroplasty to approximately 30–50% for irrigation and debridement procedures [2,3]. Moreover, the treatment success rate of PJI has not experienced any substantial improvement over the past two decades [4]. Given the significant harm it causes, considerable effort has been devoted to understanding its pathological processes, as evidenced by the nearly thirty-fold increase in PJI-related publications between 2001 and 2021 [5].

Recently, there has been a growing focus on the critical role of the immune system in infection defense and bone homeostasis [6,7]. Biofilm formation in PJI could help pathogens resist antibiotics and evade the host immune response, making PJI eradication more difficult [8,9]. The combination of a prosthesis and infection can complicate the immune response. Therefore, understanding the immune system's involvement in PJI has emerged as a challenging yet promising research field. Korn et al. [10] analyzed the immune cell composition of joint fluid using high-dimensional flow cytometry and found it to be a promising PJI screening tool. Furthermore, soluble immunomodulatory markers such as sCD28, sCD80, sCTLA-4, and sBTLA were identified as potential diagnostic and therapeutic markers for PJI [11]. More recently, Fisher et al. [12] performed bioinformatic prediction on immune cell profiles using RNA sequencing results from synovial fluid. However, all of the aforementioned studies focused on joint fluid, neglecting the fact that dry aspiration occurs in nearly half of the hips, which hinders the generalization of these immunologic findings [13]. Investigating the PJI immune microenvironment using periprosthetic tissues offers a promising alternative; however, relevant studies are still lacking. Further evaluation of the contribution of the immune system in different lesion samples could provide additional insight into the diagnosis and treatment of PJI.

In the present study, we aimed to identify immune-related genes (IRGs) in the periprosthetic tissues of patients with PJI using bioinformatics approaches and to investigate potential associations between hub genes and immune infiltration patterns. The results of our research will establish a foundation for a deeper understanding of the immune response associated with PJI.

2. Material and methods

2.1. Data preparation

Fig. 1 depicts the workflow of the present study. The gene expression data of periprosthetic tissue (GSE7103) were obtained from the Gene Expression Omnibus (GEO) repository. It included ten periprosthetic tissue samples from five patients with aseptic loosening [one woman/four men; mean age 70 years (range, 58–81 years)] and five patients with PJI [four women/one man; mean age 70 years (range, 57–88 years); *Streptococcus orales* was detected in one patient, *Staphylococcus aureus* in two, and *Staphylococcus epidermidis* in two]. Detailed demographic information is presented in Table S1. There were no statistically significant differences in age (Mann-

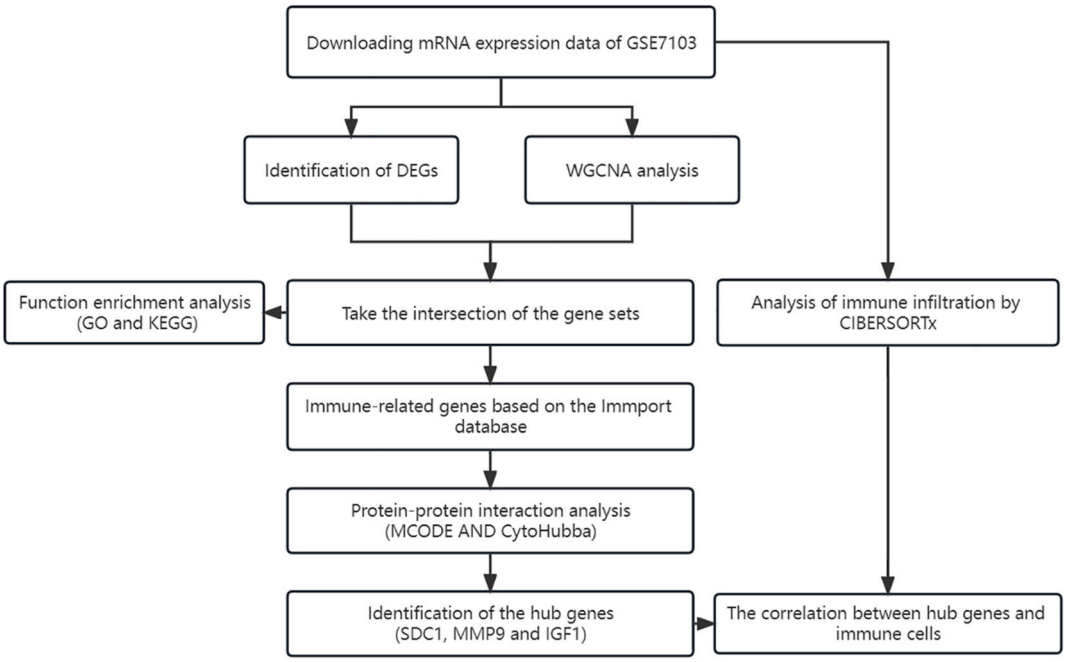

Fig. 1. The workflow of the present study.

Whitney U test, $p = 0.917$, $Z = -0.105$) or sex (Fisher's exact test, $p = 0.206$) between the two groups. These ten patients primarily received cemented total hip arthroplasty with metal-on-polyethylene bearings because of osteoarthritis. Then, the gene expression matrix was preprocessed, and the "probe ids" were configured into "symbols" using the gene annotation file obtained from GENCODE. Missing values were filled using the "impute.knn" function from the "impute" package. If a probe matched multiple genes, it was removed; and if multi-probes matched one gene, the average was taken. The data were further normalized using the "normalizeBetweenArrays" function from the "limma" package and then log-transformed. The normalized matrix file was provided as **Appendix A**.

2.2. Identification of differentially expressed genes (DEGs)

The DEGs between the control (aseptic loosening) and PJI groups were screened using the R package "limma", which was based on linear model modeling. The screening criteria were defined as $|\log_2$ fold change (FC)$| > 1$ and adjusted $p < 0.05$. Furthermore, the DEGs were visualized by volcano and heat plots.

2.3. Weighted gene co-expression network analysis (WGCNA)

We used the "WGCNA" package to explore the gene interactions and identify potential modules associated with PJI [14]. The correlation adjacency matrix was constructed and outliers were removed. Additionally, the "pickSoftThreshold" function was employed to calculate the adjacency based on the soft threshold power β and convert it into a topological overlap matrix. Modules were detected by hierarchical cluster analysis and the dynamic tree-cutting algorithm. Consistent with previous studies [15,16], the abline was set to 0.25 to merge similar modules on the clustering tree. Subsequently, the gene significance (GS) and module membership (MM) of the modules were assessed. Eventually, the eigengene network was visualized. The genes that overlapped between the significant module of identified by WGCNA and the DEGs were considered as common genes (CGs).

2.4. Functional enrichment analysis and pathway enrichment analysis

The well-established DAVID [17] and KOBAS [18] databases were selected for gene ontology (GO) and Kyoto Encyclopedia of Genes and Genomes (KEGG) pathway enrichment analysis associated with CGs. The GO analysis included three components: biological process (BP), cellular component (CC), and molecular function (MF). The top five most significant GO and KEGG terms were visualized.

2.5. Transcription factors prediction

The ChEA3 tool was utilized to predict transcription factors for CGs [19]. The integrated MeanRank method was used to rank the transcription factors, as it considered results from all libraries, with lower scores indicating higher relevance.

2.6. Determination of IRGs and construction of protein-protein interaction (PPI) networks

The ImmPort is widely regarded as one of the most comprehensive collections of human immunology databases [20]. In order to obtain PJI-related IRGs, the CGs were matched to 2483 genes in the ImmPort database. The STRING database was used to develop an immune-related PPI network for IRGs with an interaction score of ≥ 0.4 as the threshold. The PPI network was visualized using Cytoscape and the core network was identified via the MCODE plugin [21]. Subsequently, the hub genes of the PPI network were detected using cytoHubba [22].

2.7. Assessment of immune cell infiltration

The CIBERSORT was employed for immune cell infiltration analysis. The LM22 dataset from this public platform was used as a signature matrix, consisting of 547 immune cell signature genes that allow the identification of 22 human immune cells in the microenvironment [23]. One thousand permutations were performed to predict the absolute abundance of various immune cells, while the relative abundance was also calculated. The correlation between different immune cell functions was assessed. Additionally, principal component analysis (PCA) was conducted for the composition of immune infiltrating cells.

2.8. Association between hub genes and infiltrating immune cells

To further investigate the potential association between key genes and immune cells, we performed Spearman correlation analysis using the "cor.test" function to examine the correlation between gene expression and immune cell abundance.

2.9. Statistical analysis

All statistical analyses in this study were performed using R software (version 4.1.0). The Mann-Whitney U test and Fisher's exact test were used to detect differences in demographics between PJI and control groups. GO and KEGG enrichment analyses were performed by hypergeometric distribution tests using the DAVID and KOBAS databases. The adjusted p-value threshold was set at 0.05,

and the gene number threshold was set at three. The top five items in each category were displayed. All statistical tests were two-tailed and *p*-values less than 0.05 were considered to indicate statistical significance. Moderately and strongly correlated were defined as r values greater than 0.7 and 0.9, respectively, in the correlation analyses.

3. Results

3.1. Identification of DEGs

Six hundred and sixty-seven DEGs, including 357 upregulated and 310 downregulated genes, were identified between PJI and control groups. The volcano (Fig. 2A) and heat (Fig. 2B) plots demonstrate significant differences in gene expression between two groups. The top five most significantly up-regulated genes were *CHIT1* ($\log_2$ FC = 6.74), *TMEM255A* ($\log_2$ FC = 5.98), *MCOLN3* ($\log_2$ FC = 4.54), *SLC47A1* ($\log_2$ FC = 4.26), and *INSM1* ($\log_2$ FC = 4.17), while the top five down-regulated genes were *IGKV1OR2-108* ($\log_2$ FC = −5.84), *MLIP* ($\log_2$ FC = −4.88), *EGFL6* ($\log_2$ FC = −4.20), *TBX3* ($\log_2$ FC = −3.88), and *IGK* ($\log_2$ FC = −3.86). Summary statistics of the DEGs are presented in Table S2.

3.2. WGCNA and identification of modules

Genes with more than 25% variation across samples in the normalized expression dataset were imported into WGCNA. We found eight modules consisting of genes with similar co-expression profiles by creating a cluster dendrogram and merging similar modules (Fig. 3A). The WGCNA analysis allowed us to further explore the correlations between different modules and clinical phenotypes. Among these modules, the turquoise module exhibited the highest positive correlation with PJI and was the only statistically significant module (r = 0.94; p = 5E-5, Fig. 3B). Consequently, the turquoise module, which contained 1847 genes, was established as the PJI-associated module. Correlation analysis revealed a strong positive correlation between MM and GS in this module (cor = 0.94, $p <$ 1e−200, Fig. 3C). Then, we got 432 CGs by crossing DEGs with genes in the PJI-associated module (Fig. 3D).

3.3. Enrichment analyses and transcription factors prediction of the CGs

Enrichment analyses were performed to discover the underlying biological functions and pathways of PJI-associated genes in periprosthetic tissues (Fig. 4A). The GO analysis revealed that the CGs were predominantly enriched in signal transduction, integrin−mediated signaling pathway, adaptive immune response, cell adhesion, and extracellular matrix organization for BP; extracellular region, integral component of the plasma membrane, extracellular exosome, plasma membrane, and extracellular space for CC; proteoglycan binding, amino acid binding, receptor binding, collagen binding, and integrin binding for MF. Many CGs were involved in two or more immune-related GO terms, suggesting that they were closely related to immune response (Fig. 4B). Additional KEGG pathway analysis revealed enrichment for the Rap1 signaling pathway, lysosome, and phagosome.

The top 10 potential transcription factors are listed in Table S5 and the contribution of each library to the integrated ranks is shown in Fig. S1. TFEC (score = 5.3), SPI1 (score = 13.2), and TWIST2 (score = 18.5) were the top three most significant transcription factors.

3.4. Construction of immune-related PPI networks and identification of hub genes

After matching genes with those in the ImmPort database and removing isolated nodes, the immune-related PPI network comprised

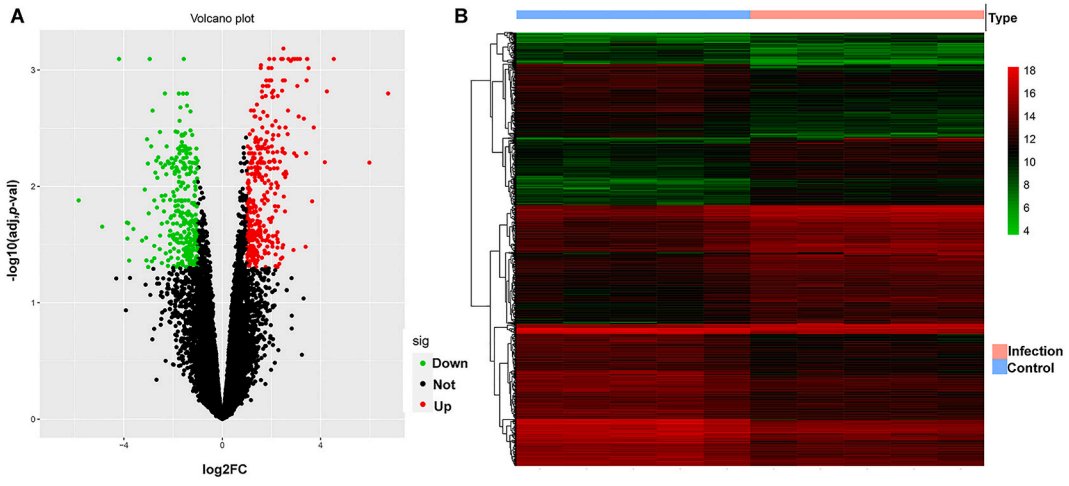

Fig. 2. Volcano (A) and heat (B) plots for the DEGs identified from GSE7103. DEG, differentially expressed gene.

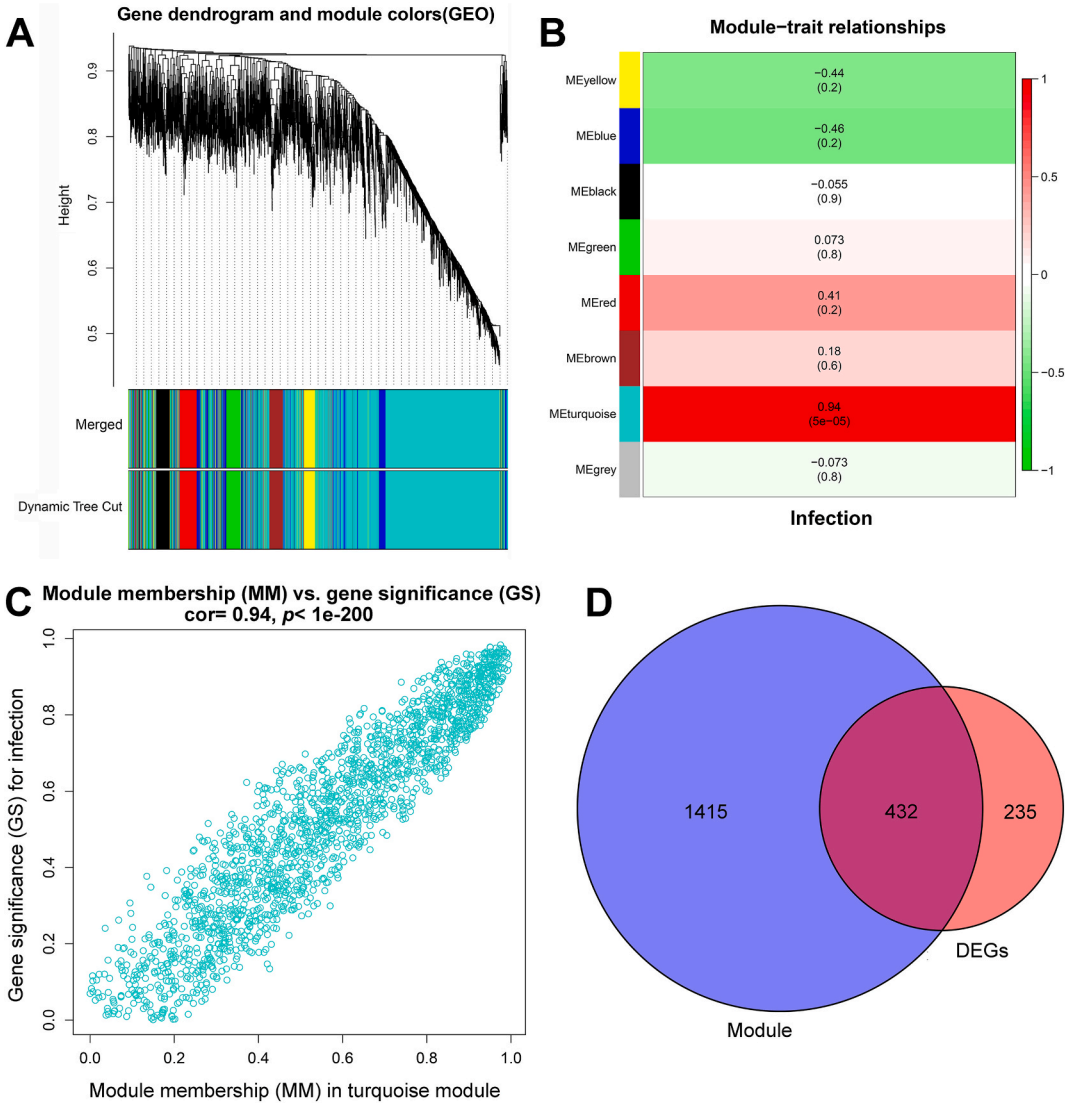

Fig. 3. Weighted gene co-expression network analysis. (A) Different colors indicate gene co-expression modules under the gene tree. (B) The turquoise module is significantly correlated with PJI. Numbers in and out of parentheses represent p-values and correlation coefficients, respectively. (C) A strong correlation between module memberships (X-axis) and gene significance (Y-axis). (D) Venn diagram indicating the common genes between DEGs and turquoise module genes. PJI, periprosthetic joint infection; DEG, differentially expressed gene. (For interpretation of the references to color in this figure legend, the reader is referred to the Web version of this article.)

of 30 upregulated and 20 downregulated nodes (Fig. 5A). Using the MCODE plugin, a core cluster consisting of 16 nodes and 53 edges was obtained (Fig. 5B). Detailed information for each cluster is provided in Table S3. We then evaluated the scores of each node by the MCC algorithm in the cytoHubba plugin, and *SDC1*, *MMP9*, and *IGF1* were identified as potential hub genes (Table S4).

3.5. Immune cell infiltration analysis

The infiltration abundance of eosinophils was found to be zero. Consequently, we proceeded to assess the infiltration of the other 21 immune cells. The bar plot (Fig. 6) illustrates the infiltration pattern of these 21 immune cells in each periprosthetic tissue sample, with different colors indicating the proportion of immune cells. It was evident that macrophages were the predominant infiltrating immune cells. Besides, the violin plot indicated higher concentrations of plasma cells ($p = 0.011$, $Z = -2.643$), CD4 memory resting T cells ($p = 0.010$, $Z = -2.649$), resting mast cells ($p = 0.008$, $Z = -2.611$), neutrophils ($p = 0.005$, $Z = -2.009$), and follicular helper T cells ($p = 0.016$, $Z = -2.403$) in PJI samples, while lower concentrations of M0 macrophages were observed ($p = 0.008$, $Z = -2.611$, Fig. 7A). Correlation analysis demonstrated that the most significant positive correlations were found between neutrophils and dendritic cells activated (cor = 0.98), CD8 T cells and M1 macrophages (cor = 0.93), whereas negative associations were found between resting mast

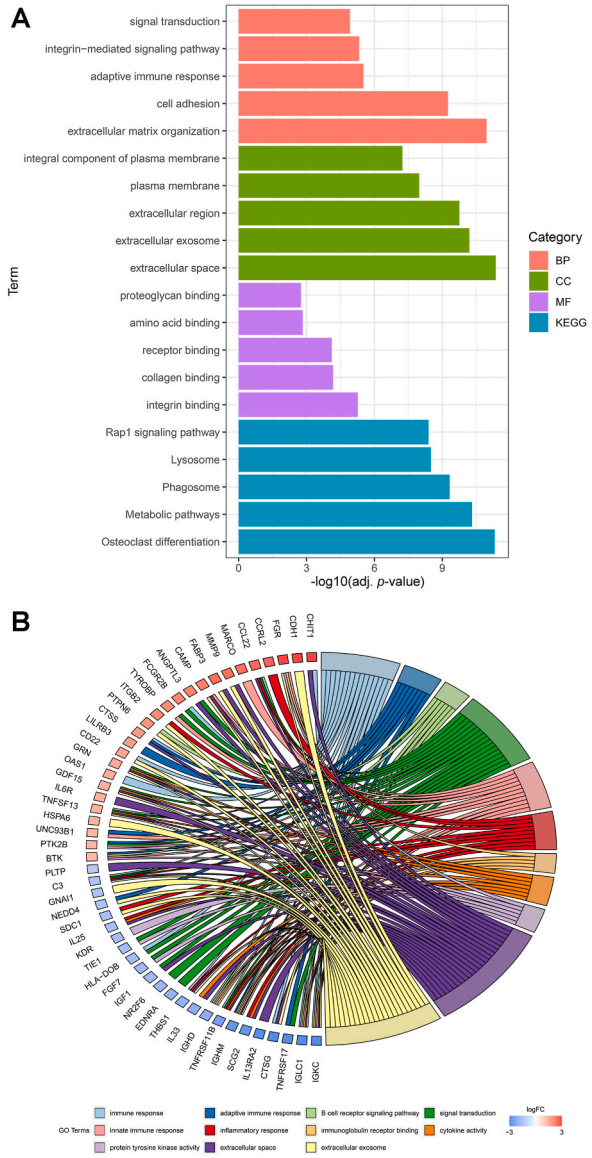

Fig. 4. (A) The top five terms of the Gene Ontology (GO) and the Kyoto Encyclopedia of Genes and Genomes (KEGG) pathway analysis. The GO terms involved three components: biological process (BP), cellular component (CC), and molecular function (MF). (B) The chord plot shows the close association between immune-related GO items and common genes.

cells and M0 macrophages (cor = 0.94), and between follicular helper T cells and M0 macrophages (cor = 0.93, Fig. 7B). Moreover, the PJI cases can be distinguished by PCA analysis according to their immune cell composition (Fig. 7C).

3.6. Correlation of hub genes and immune cells

The levels of *SDC1*, *MMP9*, and *IGF1* were found to correlate with the abundance of seven different immune cells. *SDC1* exhibited a negative correlation with resting mast cells, M1 macrophages, plasma cells, follicular helper T cells, CD8 T cells, and CD4 memory resting T cells, but a positive correlation with M0 macrophages (Fig. 8A). *MMP9* expression was positively correlated with neutrophils, follicular helper T cells, plasma cells, monocytes, resting mast cells, and CD8 T cells, but negatively correlated with M0 macrophages (Fig. 8B). *IGF1* was negatively correlated with CD8 T cells, follicular helper T cells, M1 macrophages, resting mast cells, CD4 memory resting T cells, and plasma cells, but positively correlated with M0 macrophages (Fig. 8C).

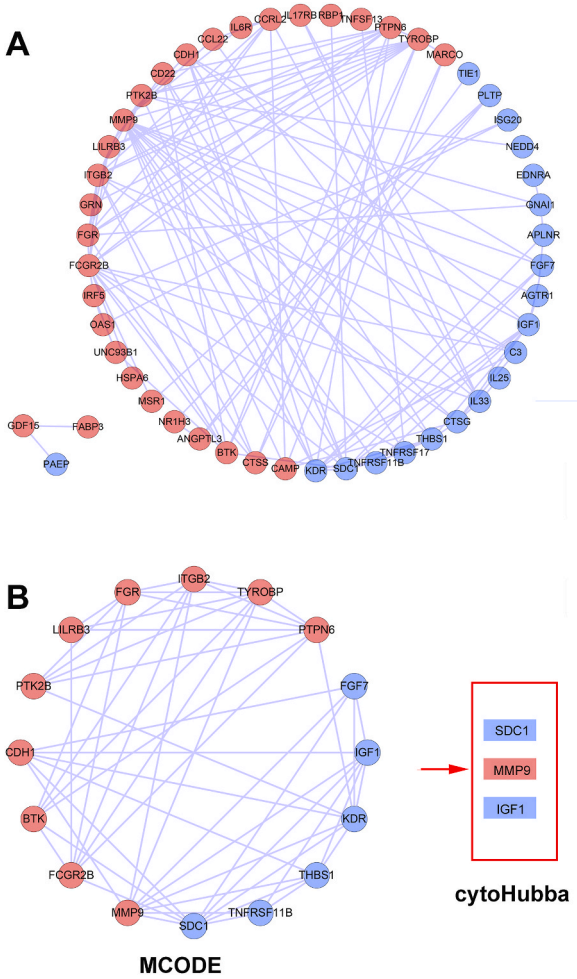

Fig. 5. (A) Immune-related protein-protein interaction network. (B) Identification of core networks by MCODE and subsequently screening of hub genes by cytoHubba. Red nodes indicate up-regulated genes, while blue nodes indicate down-regulated genes. (For interpretation of the references to color in this figure legend, the reader is referred to the Web version of this article.)

4. Discussion

PJI is a rare but catastrophic complication following TJA, which imposes a substantial burden on the healthcare system due to its high cost and tendency to reoccur [1]. Although the understanding of the molecular mechanisms underlying PJI is limited, recent studies have suggested that immune pathways may play a critical role in PJI, and the identification of novel immune-related profiles could lead to the development of new diagnostic and therapeutic strategies [6,9,12,24]. To the best of our knowledge, the present research represents the first investigation of immune cell infiltration patterns in periprosthetic tissues of PJI. In general, 667 DEGs were identified, and 1847 PJI-related module genes were obtained in WGCNA. Enrichment analysis revealed that these common genes were mainly enriched in immune and host defense-related terms. Higher levels of plasma cells, $CD4^{+}$ memory resting T cells, follicular helper T cells, resting mast cells, and neutrophils were found in PJI group, while levels of M0 macrophages were lower. Moreover, *SDC1*, *MMP9*, and *IGF1* were identified as potential immune-related biomarkers using a series of bioinformatics approaches. These findings could greatly contribute to our understanding of novel immune-related signatures in PJI.

Our enrichment analyses identified several immune-related terms. Apart from adaptive immune responses, integrin-mediated signaling pathways and integrin binding were also significantly enriched. The critical role of integrins in immune regulation has been well investigated and could be responsible for the recruitment of lymphocytes from lymph nodes to sites of infection or inflammation [25–29]. Integrin activation has been proven to be an essential component of several infections, including SARS-CoV-2, human immunodeficiency virus (HIV), and human papillomavirus [30–32]. T lymphocyte-expressed integrins can mediate communication between T cells and other cells, as well as regulate signaling. Our study further validates prior findings that the development of PJI involves an immune response, which is consistent with our research objective.

Transcription factors are key regulators of gene expression. TFEC is highly specifically expressed in macrophages [33] and can form a positive IL-4/TFEC/IL-4R feedback to promote M2 polarization. Recent research has shown that TFEC upregulation, induced by PJI,

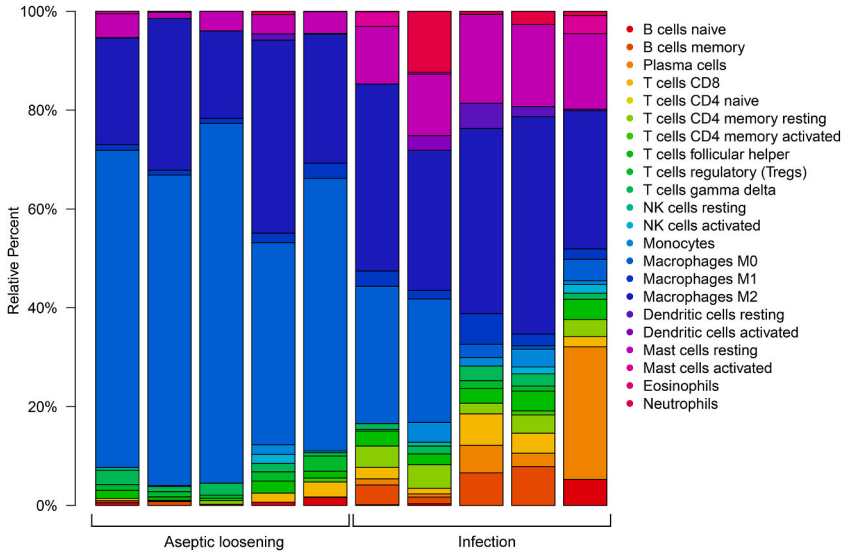

Fig. 6. The bar plot shows the composition of the 21 types of infiltrating immune cells in each sample.

can lead to inflammatory fibroblast differentiation, thereby triggering immune cell migration [34]. Additionally, SPI1 has been demonstrated to be closely associated with tumor cell survival and growth [35]. Another study found that SPI1 was also a potential core gene in the peripheral blood of sepsis patients, and its high expression increased the patient mortality [36]. TWIST2, a basic helix-loop-helix transcription factor, is involved in bone development [37] and can attenuate the inflammatory response in infant pneumonia via the NLRP3 inflammasome [38]. These findings suggest that these transcription factors may play a significant role in inflammatory and immune functions in PJI.

Although the significant infiltration of leukocytes, particularly neutrophils, in PJI is well documented, knowledge of other immune cell profiles in PJI remains limited. The CIBERSORT analysis revealed that PJI samples had higher concentrations of plasma cells, CD4 memory resting T cells, resting mast cells, neutrophils, follicular helper T cells, and lower concentrations of M0 macrophages. Conversely, a previous study that relied on sonicate fluid yielded slightly different results. It predicted higher levels of neutrophils, activated mast cells, CD8 T cells, eosinophils, resting NK cells, and activated CD4 memory T cells in PJI cases, while the aseptic failure group had higher levels of M0 macrophages, M2 macrophages, plasma cells, regulatory T cells, naive B cells, and follicular helper T cells [12]. The reason for this discrepancy is unclear. A potential explanation is that immune infiltration in PJI may be tissue specific, and different immune cell infiltration profiles may be present in different samples. Another possible explanation could be the heterogeneity among PJI samples, which may be caused by pathogenic bacteria, duration of infection, etc. Identifying such differences could improve our understanding of the immune alterations in PJI. In particular, the infiltration of mast cells in PJI tissues is an intriguing but uncharacterized issue. Tissue-resident mast cells could secrete antimicrobial peptides, recruit neutrophils, and participate in antigen presentation to mediate antimicrobial inflammation, possibly acting as a type of sentinel cell [39,40]. Furthermore, the activation of joint-specific mast cells was also associated with enhanced inflammation [41]. These findings emphasize the crucial function of mast cells in the immune response to PJI.

Although immunotherapy is a promising therapeutic strategy for chronic implant-related infections, there is a severe paucity of immune-related markers for PJI. In this study, we have identified *SDC1*, *MMP9*, and *IGF1* as potential PJI markers for the first time. SDC1, a major proteoglycan present in epithelial cells, is targeted by numerous pathogens during the initial stages of pathogenesis [42]. Some pathogens can bind to SDC1 heparan sulfate to facilitate attachment and internalization [43]. In addition, SDC1 has been shown to facilitate infection progression by shedding extraterritorial domains and suppressing innate defense mechanisms [44,45]. Previous studies have also focused on the role of SDC1 in the endothelial glycocalyx [46], which can be degraded in sepsis by inflammation-related mechanisms such as metalloproteinases [47]. Studies on sepsis have shown a correlation between blood levels of glycocalyx components and disease severity or mortality [48–50]. Additional investigation on the role of *SDC1* in PJI may provide more valuable insights. In addition, mining the associations between these potential markers and immune cell infiltration could assist us in understanding their function in the immune microenvironment. Our analysis revealed a strong positive correlation between *SDC1* expression and resting mast cells. Although few previous studies have investigated their relationship, a recent study found that both *SDC1* and resting mast cell levels may be prognostic factors for patients with glioblastoma [51]. Furthermore, the strongest negative correlation between *SDC1* and macrophages M0 was observed in our study. In contrast, there was a strong positive correlation between them in aortic valve calcification [52]. More data would be needed to interpret these findings, and further investigation of the role of *SDC1* in PJI may provide more valuable insights.

MMP9 is an essential regulator of neutrophil migration and plays a role in maintaining the dynamic homeostasis of the extracellular matrix. It is involved in various pathological processes [53]. Although its specific role in PJI remains unclear, several studies have reported its potential as a biomarker for sepsis [54–56]. Besides, matrix metalloproteinases can interact with integrin receptors on the

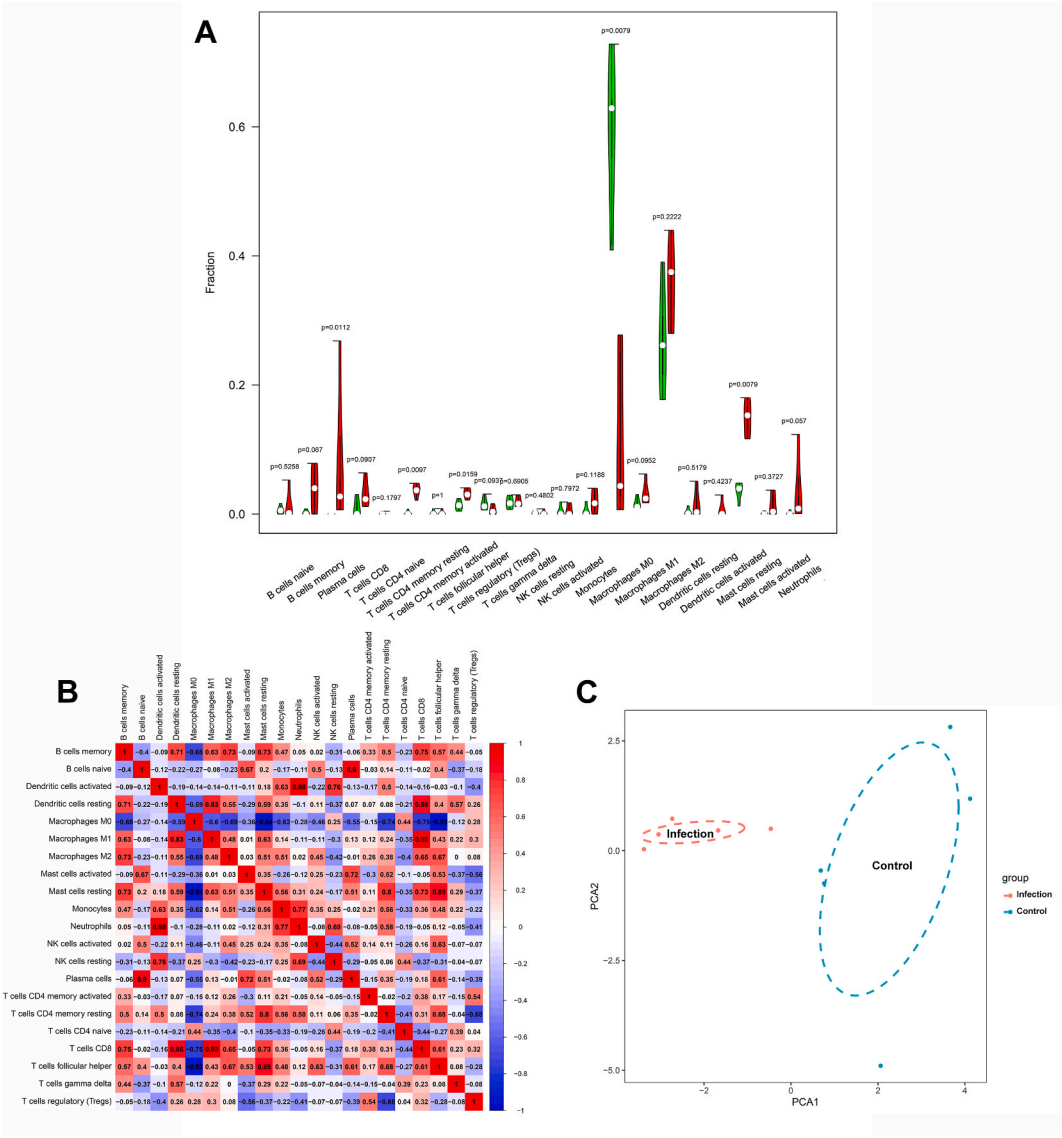

Fig. 7. Visualization and comparison of immune cell infiltration. (A) The violin plot demonstrates the difference in immune cell subtypes between the PJI and control groups. Green and red represent control and PJI group samples, respectively. (B) The correlation heat map of immune cells. (C) PCA analysis can distinguish PJI from controls based on the composition of infiltrating immune cells. PJI, periprosthetic joint infection. (For interpretation of the references to color in this figure legend, the reader is referred to the Web version of this article.)

cell surface to promote the migration of inflammatory cells to the site of infection. In a murine model, Daghighi et al. observed that *Mmp* and integrins were upregulated when both pathogenic bacteria and implants were present, while the immune system was still struggling to eradicate the infection [57]. The aforementioned findings highlight the potential of *MMP9* as a novel marker for infectious diseases. Correlation analysis revealed that the immune cells most positively correlated with *MMP9* were macrophages M0. Macrophage morphological plasticity and migration were Rac signaling and *MMP9* dependent [58]. Recent studies have shown that macrophage-derived MMP9 can induce the development of various diseases such as renal fibrosis and cerebral aneurysms [59,60]. Our results highlighted their potential role in PJI. Neutrophils could release MMP9 to promote angiogenesis and tumor cell dissemination [61]. Neutrophil extracellular traps were also enriched with high levels of MMP9 and neutrophil elastase [62]. However, a negative correlation between *MMP9* expression and neutrophils was found in PJI. The reasons for this phenomenon remain to be investigated.

IGF1 plays a significant role in regulating bone remodeling and metabolism, and is critical for preserving bone density throughout an individual's lifespan [63]. A recent study revealed a close association between reduced IGF1 levels and the development of osteoporosis and sarcopenia in the elderly [64]. In addition, it has emerged as a potential biomarker for postmenopausal osteoporosis [65]. Infectious osteomyelitis can induce secondary osteoporosis by affecting osteoclast function, and the infected bone loss has recently been proven to be present in PJI [66,67]. However, bone mass in PJI patients has not received much attention [67]. Hence, there is an

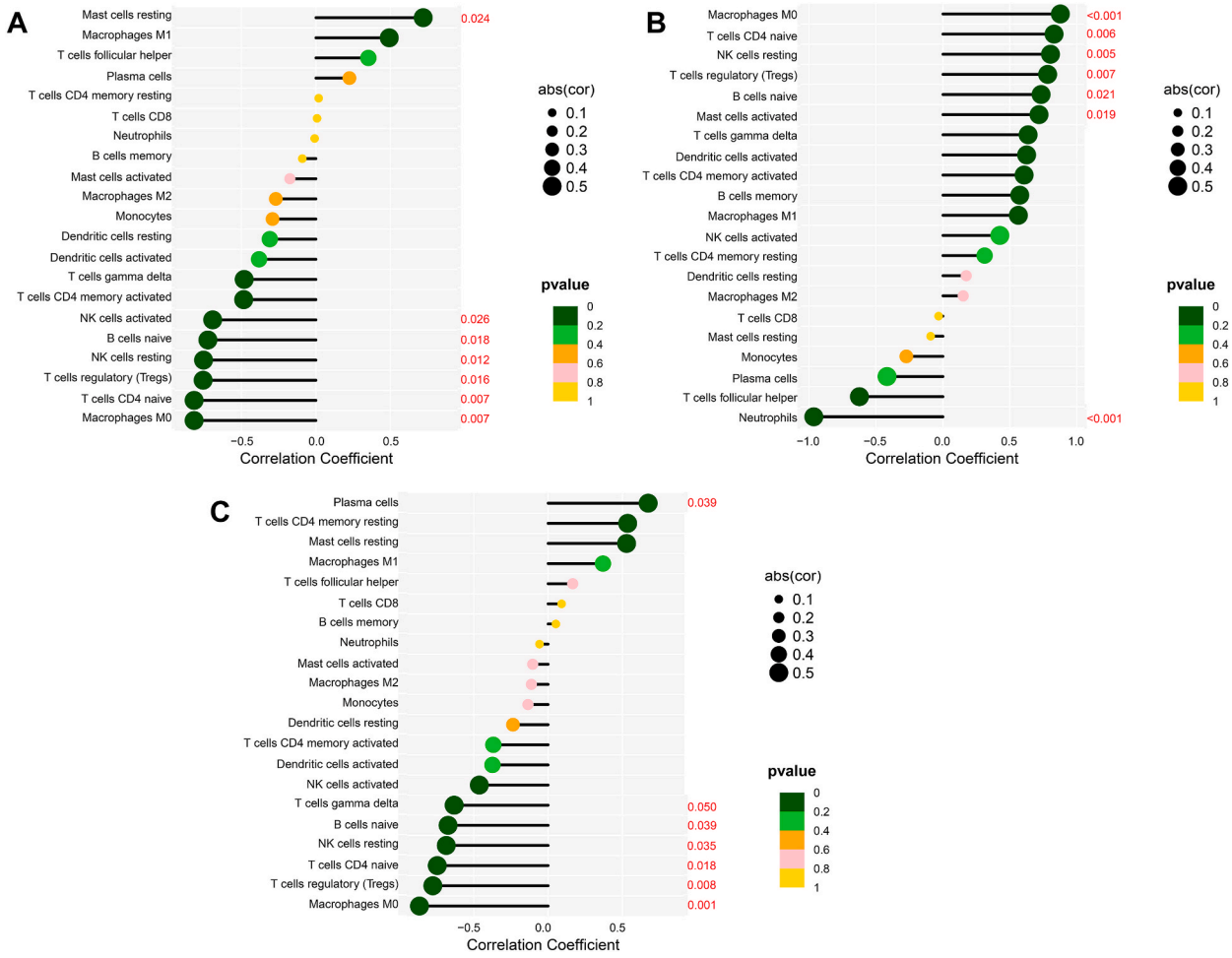

Fig. 8. Correlation between SDC1 (A), MMP9 (B), or IGF1 (C) and infiltrating immune cells.

immediate requirement for more comprehensive research to explore the clinical significance of infection-induced osteolysis in PJI. In the present study, *IGF1* was found to be positively correlated with plasma cells and negatively correlated with macrophages M0. It was demonstrated that *IGF1* can mediate proliferative and anti-apoptotic signaling in plasma cells [68]. These data suggested their potential synergistic role in the development of PJI. In addition, *IGF1* and macrophages M0 were simultaneously identified as immune-related molecular prognostic indicators in bladder cancer [69]. In HIV-infected patients, *IGF1* and monocyte/macrophage activation markers (sCD163, sCD14) were negatively correlated [70]. Therefore, future studies should investigate the mechanisms and prognostic significance of these molecular markers in PJI.

Several limitations should be noted when interpreting our findings. First, only one dataset was used for the bioinformatic analysis. However, PJI-related datasets were scarce, making our results an important foundation for future immune-related studies of PJI. Second, the small sample size of the present study prevented us from assessing the effect of confounding factors such as age and gender on gene expression and immune infiltration levels. Third, specific inclusion or exclusion criteria for patient selection remained unclear. Fourth, we did not find statistical differences in most immune cell types. This may be due to the considerable heterogeneity among PJI patients, and the present sample size was insufficient to detect potential differences. In addition, patient medication history, such as systemic or topical antibiotic administration, was not available, and information on risk factors for PJI, such as smoking, alcohol consumption, and local soft tissue disease [71,72], was lacking, making it impossible for us to assess their potential impact. Therefore, larger and more detailed studies would be needed to more comprehensively investigate the immune microenvironment in patients with PJI. Finally, future in vitro and in vivo experiments are still needed to validate the findings of our study.

5. Conclusion

In conclusion, the present study unveiled, for the first time, immune infiltration signatures in PJI periprosthetic tissues. Three hub genes, *SDC1*, *MMP9*, and *IGF1*, were identified as potential novel immune-related biomarkers for PJI. Our findings could provide a basis for researchers to gain a deeper understanding of the immune response associated with the development of PJI.

Ethics approval and informed consent

This study did not include any patient information. Thus, the requirement for ethics approval was waived.

Data availability statement

The data for this study can be obtained from the GEO database.

CRediT authorship contribution statement

Zhuo Li: Writing – review & editing, Writing – original draft, Visualization, Software, Methodology, Investigation, Formal analysis, Data curation, Conceptualization. **Zhi-Yuan Li:** Writing – review & editing, Validation, Methodology, Investigation, Formal analysis. **Zulipikaer Maimaiti:** Writing – original draft, Software, Resources, Investigation, Formal analysis, Data curation. **Fan Yang:** Visualization, Validation, Software, Investigation. **Jun Fu:** Writing – review & editing, Writing – original draft, Resources, Project administration, Methodology, Funding acquisition. **Li-Bo Hao:** Writing – review & editing, Writing – original draft, Software, Resources, Investigation. **Ji-Ying Chen:** Writing – review & editing, Writing – original draft, Visualization, Supervision, Conceptualization. **Chi Xu:** Writing – review & editing, Writing – original draft, Methodology, Investigation, Funding acquisition, Conceptualization.

Declaration of competing interest

The authors declare that they have no known competing financial interests or personal relationships that could have appeared to influence the work reported in this paper.

Acknowledgements

This work was supported by the National Key Research and Development Program of China (No. 2020YFC2004900, 2023YFB4705600), the National Natural Science Foundation of China (No.82002323, 82102585), and the Military Medical Science and Technology Youth Training Project (No.21QNPY110).

Appendix A. Supplementary data

Supplementary data to this article can be found online at https://doi.org/10.1016/j.heliyon.2024.e26062.

References

[1] A.J. Tande, R. Patel, Prosthetic joint infection, Clin. Microbiol. Rev. 27 (2) (2014) 302–345.
[2] A.J. Bryan, et al., Irrigation and debridement with component Retention for acute infection after hip arthroplasty: Improved results with Contemporary Management, J Bone Joint Surg Am 99 (23) (2017) 2011–2018.
[3] S.R. Nodzo, et al., Success rates, characteristics, and costs of articulating antibiotic spacers for total knee periprosthetic joint infection, Knee 24 (5) (2017) 1175–1181.
[4] C. Xu, et al., Is treatment of periprosthetic joint infection improving over time? J. Arthroplasty 35 (6) (2020) 1696–1702 e1.
[5] C.R. Fisher, R. Patel, Profiling the immune response to periprosthetic joint infection and Non-infectious arthroplasty failure, Antibiotics (Basel) 12 (2) (2023).
[6] E. Seebach, K.F. Kubatzky, Chronic implant-related bone infections-can immune Modulation be a therapeutic strategy? Front. Immunol. 10 (2019) 1724.
[7] Z. Li, et al., The superiority of immune-inflammation summary index for diagnosing periprosthetic joint infection, Int. Immunopharm. 118 (2023) 110073.
[8] C.R. Arciola, D. Campoccia, L. Montanaro, Implant infections: adhesion, biofilm formation and immune evasion, Nat. Rev. Microbiol. 16 (7) (2018) 397–409.
[9] B.F. Ricciardi, et al., Staphylococcus aureus evasion of host Immunity in the Setting of prosthetic joint infection: biofilm and beyond, Curr Rev Musculoskelet Med 11 (3) (2018) 389–400.
[10] M.F. Korn, et al., High-dimensional analysis of immune cell composition predicts periprosthetic joint infections and Dissects its Pathophysiology, Biomedicines 8 (9) (2020).
[11] J.M. Jubel, et al., sCD28, sCD80, sCTLA-4, and sBTLA are promising markers in diagnostic and therapeutic approaches for aseptic loosening and periprosthetic joint infection, Front. Immunol. 12 (2021) 687065.
[12] C.R. Fisher, et al., Sonicate fluid Cellularity predicted by transcriptomic Deconvolution differentiates infectious from non-infectious arthroplasty failure, J Bone Joint Surg Am 105 (1) (2023) 63–73.
[13] D.G. Partridge, et al., Joint aspiration, including culture of reaspirated saline after a 'dry tap', is sensitive and specific for the diagnosis of hip and knee prosthetic joint infection, Bone Joint Lett. J 100-B (6) (2018) 749–754.
[14] P. Langfelder, S. Horvath, WGCNA: an R package for weighted correlation network analysis, BMC Bioinf. 9 (2008) 559.
[15] C. Wei, et al., Identification and verification of diagnostic biomarkers in recurrent pregnancy loss via machine learning algorithm and WGCNA, Front. Immunol. 14 (2023) 1241816.
[16] S. Xiao, et al., Uncovering potential novel biomarkers and immune infiltration characteristics in persistent atrial fibrillation using integrated bioinformatics analysis, Math. Biosci. Eng. 18 (4) (2021) 4696–4712.
[17] W. Huang da, B.T. Sherman, R.A. Lempicki, Systematic and integrative analysis of large gene lists using DAVID bioinformatics resources, Nat. Protoc. 4 (1) (2009) 44–57.
[18] J. Wu, et al., KOBAS server: a web-based platform for automated annotation and pathway identification, Nucleic Acids Res. 34 (2006) W720–W724 (Web Server issue).

[19] A.B. Keenan, et al., ChEA3: transcription factor enrichment analysis by orthogonal omics integration, Nucleic Acids Res. 47 (W1) (2019) W212–W224.
[20] S. Bhattacharya, et al., ImmPort, toward repurposing of open access immunological assay data for translational and clinical research, Sci. Data 5 (2018) 180015.
[21] P. Shannon, et al., Cytoscape: a software environment for integrated models of biomolecular interaction networks, Genome Res. 13 (11) (2003) 2498–2504.
[22] C.H. Chin, et al., cytoHubba: identifying hub objects and sub-networks from complex interactome, BMC Syst. Biol. 8 (Suppl 4) (2014) S11. Suppl 4.
[23] A.M. Newman, et al., Robust enumeration of cell subsets from tissue expression profiles, Nat. Methods 12 (5) (2015) 453–457.
[24] Z. Li, et al., Moderate-to-Severe malnutrition identified by the controlling nutritional status (CONUT) score is significantly associated with treatment failure of periprosthetic joint infection, Nutrients 14 (20) (2022).
[25] D.S. Heffernan, S.F. Monaghan, A. Ayala, Lymphocyte integrin expression differences between SIRS and sepsis patients, Ir. J. Med. Sci. 186 (4) (2017) 981–987.
[26] I. Mitroulis, et al., Leukocyte integrins: role in leukocyte recruitment and as therapeutic targets in inflammatory disease, Pharmacol. Ther. 147 (2015) 123–135.
[27] S. Nourshargh, R. Alon, Leukocyte migration into inflamed tissues, Immunity 41 (5) (2014) 694–707.
[28] Y. Zhang, H. Wang, Integrin signalling and function in immune cells, Immunology 135 (4) (2012) 268–275.
[29] O.J. Mezu-Ndubuisi, A. Maheshwari, The role of integrins in inflammation and angiogenesis, Pediatr. Res. 89 (7) (2021) 1619–1626.
[30] P. Simons, et al., Integrin activation is an essential component of SARS-CoV-2 infection, Sci. Rep. 11 (1) (2021) 20398.
[31] Q. Liu, P. Lusso, Integrin alpha4beta7 in HIV-1 infection: a critical review, J. Leukoc. Biol. 108 (2) (2020) 627–632.
[32] P. Aksoy, et al., HPV16 infection of HaCaTs is dependent on beta4 integrin, and alpha6 integrin processing, Virology 449 (2014) 45–52.
[33] S. Kim, et al., MiT family transcriptional factors in immune cell functions, Mol Cells 44 (5) (2021) 342–355.
[34] J. Yu, et al., Single-cell transcriptome reveals Staphylococcus aureus modulating fibroblast differentiation in the bone-implant interface, Mol Med 29 (1) (2023) 35.
[35] H. Feng, et al., SPI1 is a prognostic biomarker of immune infiltration and immunotherapy efficacy in clear cell renal cell carcinoma, Discov Oncol 13 (1) (2022) 134.
[36] J. Liu, et al., Screening of potential core genes in peripheral blood of adult patients with sepsis based on transcription regulation function, Shock 59 (3) (2023) 385–392.
[37] Y. Huang, et al., Twist1- and Twist2-haploinsufficiency results in reduced bone formation, PLoS One 9 (6) (2014) e99331.
[38] N. Ding, et al., Twist2 reduced NLRP3-induced inflammation of infantile pneumonia via regulation of mitochondrial permeability transition by FOXO1, Int. Arch. Allergy Immunol. 183 (10) (2022) 1098–1113.
[39] C.F. Johnzon, E. Ronnberg, G. Pejler, The role of mast cells in bacterial infection, Am. J. Pathol. 186 (1) (2016) 4–14.
[40] A.M. Piliponsky, M. Acharya, N.J. Shubin, Mast cells in viral, bacterial, and fungal infection immunity, Int. J. Mol. Sci. 20 (12) (2019).
[41] P.A. Nigrovic, D.M. Lee, Synovial mast cells: role in acute and chronic arthritis, Immunol. Rev. 217 (2007) 19–37.
[42] R.S. Aquino, Y.H. Teng, P.W. Park, Glycobiology of syndecan-1 in bacterial infections, Biochem. Soc. Trans. 46 (2) (2018) 371–377.
[43] J. Mengaud, et al., E-cadherin is the receptor for internalin, a surface protein required for entry of L. monocytogenes into epithelial cells, Cell 84 (6) (1996) 923–932.
[44] A. Hayashida, S. Amano, P.W. Park, Syndecan-1 promotes Staphylococcus aureus corneal infection by counteracting neutrophil-mediated host defense, J. Biol. Chem. 286 (5) (2011) 3288–3297.
[45] P.W. Park, et al., Exploitation of syndecan-1 shedding by Pseudomonas aeruginosa enhances virulence, Nature 411 (6833) (2001) 98–102.
[46] B.F. Becker, et al., Degradation of the endothelial glycocalyx in clinical settings: searching for the sheddases, Br. J. Clin. Pharmacol. 80 (3) (2015) 389–402.
[47] E.P. Schmidt, et al., The pulmonary endothelial glycocalyx regulates neutrophil adhesion and lung injury during experimental sepsis, Nat Med 18 (8) (2012) 1217–1223.
[48] A. Nelson, et al., Increased levels of glycosaminoglycans during septic shock: relation to mortality and the antibacterial actions of plasma, Shock 30 (6) (2008) 623–627.
[49] J. Steppan, et al., Sepsis and major abdominal surgery lead to flaking of the endothelial glycocalix, J. Surg. Res. 165 (1) (2011) 136–141.
[50] M. Sallisalmi, et al., Vascular adhesion protein-1 and syndecan-1 in septic shock, Acta Anaesthesiol. Scand. 56 (3) (2012) 316–322.
[51] X. Chen, F. Tian, Z. Wu, A genomic instability-associated prognostic signature for glioblastoma patients, World Neurosurg 167 (2022) e515–e526.
[52] K. Huang, et al., Transcriptome sequencing data reveal LncRNA-miRNA-mRNA regulatory network in calcified aortic valve disease, Front Cardiovasc Med 9 (2022) 886995.
[53] H. Huang, Matrix metalloproteinase-9 (MMP-9) as a cancer biomarker and MMP-9 biosensors: recent advances, Sensors 18 (10) (2018).
[54] M.M. Ahmed, et al., Identification and validation of pathogenic genes in sepsis and associated diseases by integrated bioinformatics approach, Genes 13 (2) (2022).
[55] J. Liang, et al., Analysis of sepsis markers and pathogenesis based on gene differential expression and protein interaction network, J Healthc Eng 2022 (2022) 6878495.
[56] H. Deng, et al., Commonly expressed key transcriptomic profiles of sepsis in the human circulation and brain via integrated analysis, Int. Immunopharm. 104 (2022) 108518.
[57] S. Daghighi, et al., Real-time quantification of matrix metalloproteinase and integrin alphavbeta3 expression during biomaterial-associated infection in a murine model, Eur. Cell. Mater. 27 (2014) 26–37. ; discussion 37-8.
[58] J. Travnickova, et al., Macrophage morphological plasticity and migration is Rac signalling and MMP9 dependant, Sci. Rep. 11 (1) (2021) 10123.
[59] T.K. Tan, et al., Matrix metalloproteinase-9 of tubular and macrophage origin contributes to the pathogenesis of renal fibrosis via macrophage recruitment through osteopontin cleavage, Lab. Invest. 93 (4) (2013) 434–449.
[60] T. Aoki, et al., Macrophage-derived matrix metalloproteinase-2 and -9 promote the progression of cerebral aneurysms in rats, Stroke 38 (1) (2007) 162–169.
[61] L. Modestino, et al., Neutrophil extracellular traps and neutrophil-related mediators in human thyroid cancer, Front. Immunol. 14 (2023) 1167404.
[62] J. Albrengues, et al., Neutrophil extracellular traps produced during inflammation awaken dormant cancer cells in mice, Science (6409) (2018) 361.
[63] G. Mazziotti, A.G. Lania, E. Canalis, Skeletal disorders associated with the growth hormone-insulin-like growth factor 1 axis, Nat. Rev. Endocrinol. 18 (6) (2022) 353–365.
[64] R. Hata, et al., Osteoporosis and sarcopenia are associated with each other and reduced IGF1 levels are a risk for both diseases in the very old elderly, Bone 166 (2023) 116570.
[65] Y. Zhang, et al., The potential role of serum IGF-1 and leptin as biomarkers: towards screening for and diagnosing postmenopausal osteoporosis, J. Inflamm. Res. 15 (2022) 533–543.
[66] U. Dapunt, et al., Neutrophil-derived MRP-14 is up-regulated in infectious osteomyelitis and stimulates osteoclast generation, J. Leukoc. Biol. 98 (4) (2015) 575–582.
[67] T. Jiang, H. Gu, J. Wei, Echinacoside inhibits osteoclast function by down-regulating PI3K/akt/C-fos to alleviate osteolysis caused by periprosthetic joint infection, Front. Pharmacol. 13 (2022) 930053.
[68] F. Pene, et al., Role of the phosphatidylinositol 3-kinase/Akt and mTOR/P70S6-kinase pathways in the proliferation and apoptosis in multiple myeloma, Oncogene 21 (43) (2002) 6587–6597.
[69] N. Xu, et al., Development and validation of a molecular prognostic index of bladder cancer based on immunogenomic landscape analysis, Cancer Cell Int. 20 (2020) 302.
[70] L.T. Fourman, et al., Insulin-like growth factor 1 inversely relates to monocyte/macrophage activation markers in HIV, AIDS 32 (7) (2018) 927–932.
[71] H. Dale, et al., Increasing risk of prosthetic joint infection after total hip arthroplasty, Acta Orthop. 83 (5) (2012) 449–458.
[72] X. An, et al., The effect of passive smoking on early clinical outcomes after total knee arthroplasty among female patients, Risk Manag Healthc Policy 14 (2021) 2407–2419.